Strain, cell density, and nutrient condition affect patterns of diurnal vertical migration and superoxide production in a red-tide alga

Tomoyuki Shikata[1]*, Saho Kitatsuji[1] and Koki Yuasa[2]

[1]Fisheries Technology Institute, Japan Fisheries Research and Education Agency, Nagasaki, Goto, Japan,
[2]Fisheries Technology Institute, Japan Fisheries Research and Education Agency, Hiroshima, Hatsukaichi, Japan

A red tide occurs when cell densities of autotrophic microalgae and some heterotrophic protists increase dramatically and thereby change the color of the sea. Red tides sometimes have negative impacts on human activities, such as fisheries and tourism. Most red-tide flagellates display diurnal vertical migration (DVM) in which cells normally migrate upward during the day and downward at night. This behavior promotes active growth, due to the effective acquisition of nutrients and light, as well as population density increase and cell aggregation. However, the factors and their interactions influencing DVM remain to be clarified, such that no algorithm exists that can precisely simulate the DVM pattern and the development of a red tide in the field. *Chattonella* marina complex (hereafter *Chattonella*) is a representative microalga of harmful red tides and some previous studies has suggested that *Chattonella*'s DVM plays important roles in development of a red tide. *Chattonella* can produce a large amount of superoxide ($\bullet O_2^-$), which is responsible for the regulation of various physiological processes as well as its toxicity against microorganisms and animals. In the present study, we examined the effects of strain, growth phase, cell density, and nutrient deficiency on the pattern of DVM. In addition, we also measured the $\bullet O_2^-$ level in most experiments to assess the relationship between DVM and $\bullet O_2^-$ production. Some strains displayed clear DVM, whereas others aggregated at the surface all day in a fixed condition. Strains' DVM patterns did not show a relationship with $\bullet O_2^-$ production. Moreover, the DVM became less clear at high cell density and in nitrogen- or phosphorus-depleted conditions. Although a previous study reported that the $\bullet O_2^-$ production rate increased during the light period and decreased during the dark period, regardless of cell density, the diurnal pattern of $\bullet O_2^-$ became less clear at a higher cell density in a *Chattonella* strain used in the present study. Our findings indicate that DVM and $\bullet O_2^-$ production by a *Chattonella* population composed of various strains can change across developmental phases and environmental conditions. This characteristic may produce adaptability in species and increase the chances of a massive population increase.

KEYWORDS

circadian rhythm, diversity, flagellate, harmful algal bloom, interstrain difference, marine phytoplankton, raphidophyte, swimming

1 Introduction

In marine environments, cell densities of autotrophic microalgae and some heterotrophic protists increase and thereby change the color of the sea—a biological phenomenon known as a red tide. Some red tides negatively impact fisheries and tourism (Sellner et al., 2003), and the impacts of harmful red tides on coastal systems have increased in recent decades (Gobler, 2020). Techniques for mitigating damages in the fish culture industry have been suggested (Kim, 2006; Balaji-Prasath et al., 2022), with precautionary field interventions such as early harvesting, restricting fish feeding, and transport of fish cages into zones free of red tides being the most practical (Kim, 2006). To boost the effectiveness of these precautionary interventions, accurate forecasting of the arrival of a red tide at fishing grounds is necessary. Forecasting based on numerical models is challenging because the densification and expansion of a red tide are influenced by various factors, including biological, chemical, and physical processes (McGillicuddy, 2010; Davidson et al., 2016).

In most cases, the outbreak of a red tide in a marine area requires three steps. First is the appearance of cells in the area due to the transport of cells from other marine areas, growth of surviving cells at quite low density, and excystment. Next is the growth step, in which the cell division rate exceeds the loss rate. The third step is aggregation, which occurs due to physical and biological processes. Various environmental factors influence each of the three steps. As compared to the aggregation process, the growth and life-history stages (including excystment) of red-tide algae have been more thoroughly studied and reported (e.g., Granéli and Turner, 2006).

Most flagellates causing red tides display diurnal vertical migration (DVM) in which cells normally migrate upward during the day and downward at night (Kamykowski, 1995). DVM contributes greatly to the aggregation step (Lai and Yin, 2014) and likely to the growth step as well, as the process offers many ecological benefits to flagellates, such as nutrient acquisition at a wider range of depths, the ability to control the amount of light received for photosynthesis, and escape from predators (Smayda, 1997; Harvey and Menden-Deuer, 2011; Bollens et al., 2012).

Among red-tide flagellates, the DVM pattern follows the photoperiod and appears to be controlled by an endogenous clock (Roenneberg et al., 1989; Shikata et al., 2015), whereas the timing of change in swimming direction and swimming speed differ among species (Kamykowski, 1995; Shikata et al., 2015). Some studies indicated that even if the dominant species is the same across a marine area, DVM patterns can differ among places and days (Katano et al., 2014; Shikata et al., 2020). Previous studies revealed that the DVM pattern is influenced by external environmental factors such as temperature (Heaney and Eppley, 1980), salinity (Jephson et al., 2011), light (Ault, 2000), and nutrient concentrations (Heaney and Eppley, 1980). Based on their different swimming speeds, Bearon et al. (2004) postulated that DVM patterns differ among strains in a flagellate species.

Although numerical simulation models considering physical processes have been developed (Berdalet et al., 2014), no algorithm can precisely simulate DVM patterns of a red-tide algae in the field. This deficiency exists because few studies have assessed both the physical and biological processes underlying DVM, including the physiological responses to various environmental factors, and the biological parameters impacting DVM patterns remain to be clarified for each red tide flagellate.

The raphidophyte *Chattonella marina* complex (hereafter called *Chattonella*) is distributed in warm marine coastal areas around the world and has caused tremendous damage to fisheries (Imai and Yamaguchi, 2012). Reflecting these threats, a large amount of information on *Chattonella* has been gathered, particularly with regard to its growth physiology, life cycle, and interaction with other microorganisms. Field data collected before and after *Chattonella* red tides are also available for designing laboratory experiments and validating numerical models using biological parameters. In addition, studies on the DVM of *Chattonella* have been conducted as well. A field experiment using a mesocosm revealed that *Chattonella* could reach a depth of 7.5 m during DVM, and its migration speed was 0.8 m h^{-1} both upward and downward (Watanabe et al., 1995). *Chattonella* can sense weak UV and blue light, allowing it to cue its DVM to the day–night cycle (Shikata et al., 2013). Negative phototaxis was observed under a monochromatic light with UV and blue components, but the response disappeared by mixing light with longer wavelengths (Shikata et al., 2016). Although one report has noted chemotaxis toward inorganic phosphate (Ikegami et al., 1995), we also observed a clear DVM in *Chattonella* without a vertical gradient of phosphate concentration (Shikata et al., 2015). Therefore, the DVM pattern may be regulated mainly by the endogenous clock that synchronizes the photoperiod and switches between positive and negative geotaxis in *Chattonella*. However, low salinity in the upper layers arrests the upward migration of *Chattonella* (Katano et al., 2014; Shikata et al., 2014), and a field study of DVM showed that cell density in the water column might also affect DVM (Sakaguchi et al., 2017). These findings indicate that there are also factors inhibiting the DVM pattern regulated by the endogenous clock.

Chattonella can produce a large amount of superoxide ($\bullet O_2^-$) in the cell membrane and excrete it from the cell. This $\bullet O_2^-$ and hydrogen peroxide has antimicrobial activity and is a candidate toxin related to fish mortality (Oda et al., 1992), as the level of $\bullet O_2^-$ is highly correlated with toxicity to aquacultured fishes in seawater that contains *Chattonella* cells (Shikata et al., 2021). Ichthyotoxicity can disappear within a short period and only live *Chattonella* cells can kill fishes; ruptured cells and culture supernatant have no toxicity to fish (Matsusato and Kobayashi, 1974; Ishimatsu et al., 1996; Shen et al., 2010). These characteristics correspond with chemical unstableness of $\bullet O_2^-$. The amount of $\bullet O_2^-$ production is influenced by nutrient and light intensity conditions; nutrient deficiency and strong light can increase the production (Yuasa et al., 2020a; b). Moreover, *Chattonella* exhibits different $\bullet O_2^-$ production rates in the light and dark periods (Kim et al., 2005; Yuasa et al., 2020a). These results suggest that $\bullet O_2^-$ may be responsible for regulating various physiological processes with circadian rhythms.

In the present study, we examined the effects of strain, growth phase, cell density, and nutrient deficiency—factors scarcely addressed thus far—on the DVM pattern in *Chattonella*. In most experiments, we also simultaneously measured the $\bullet O_2^-$ level to investigate the potential synchronous patterns of DVM and $\bullet O_2^-$ production in this flagellate species.

TABLE 1 *Chattonella* strains used in the present study. All strains were isolated from Japanese coastal areas. In cell shape, the length:width ratio of *Chattonella antiqua*-like cells are larger than *Chattonella marina*-like cells (Shikata et al., 2021).

Strain name	Year collected	Origin	Contamination status	Shape[1]	Ichthyotoxicity[1]	References
NIES-1	1978	Harima-nada	Axenic	*C. antiqua*-like	High	1)
OP27	2010	Ariake Sea	Xenic	*C. antiqua*-like[2]	High	3)
Ago03	2013	Ago Bay	Xenic	*C. marina*-like	High	1)
Ago04	2013	Ago Bay	Xenic	*C. marina*-like	Low	1)
3KGY	2010	Yatsushiro Sea	Axenic	*C. antiqua*-like	Medium	1)

[1] Shikata et al. (2021); [2] Akita et al. (2022); [3] Wada et al. (2018).

2 Materials and methods

2.1 Culture of strains

Five clonal strains of *Chattonella* were used in this study. The dates and locations for the isolation of these strains are listed in Table 1. Two strains were axenic, and the others were not. The strains were subcultured in 50-mL Erlenmeyer flasks containing 25 mL of modified SWM-3 medium (Shikata et al., 2011) with a salinity of 32 psu at 25°C under 150 µmol photons m^{-2} s^{-1} of white fluorescent irradiation on a 12:12-h light:dark cycle (light period, 06:00 to 18:00 local time [LT]). The photosynthetic photon flux density in the incubator was measured with a Quantum Scalar Laboratory PPFD sensor (QSL-2101, Biospherical Instruments Inc., San Diego, CA, United States).

2.2 Monitoring DVM with a cylindrical aquarium

A cylindrical aquarium was used as a culture vessel to monitor DVM (Shikata et al., 2014). The aquarium (inner diameter, 5 cm; height, 90 cm) was made of acrylic, with nine sampling ports (diameter, 13 mm) at intervals of 10 cm, starting from the bottom. Each port was plugged with a silicone-rubber stopper. The aquarium was placed in a temperature-controlled room (25°C) and capped with a disc-shaped LED lamp (daylight color; INREDA, Spot-light LED, Inter IKEA Systems B.V., The Netherland). The light intensity at the surface was 250 µmol photons m^{-2} s^{-1}.

On the day prior to each experiment, we added modified SWM-3 medium and a cell suspension at 17:00–18:00 LT. The total volume of the medium and the cell suspension was adjusted to 1.6 L, and the final water depth in the aquarium was about 85 cm. Each experiment was initiated at 09:00 LT, and at 3-h intervals 5 mL of the cell suspension was sampled from the water surface or from each sampling port. Then a syringe and a needle were used to refill the aquarium from the surface and bottom sampling ports with 25 mL of fresh medium.

Yamaguchi et al. (1991) reported that the cell densities of *Chattonella* are positively correlated with *in vivo* fluorescence. Therefore, to determine the vertical distribution of cells, we measured the *in vivo* fluorescence (Brand et al., 1981) of the sample at each depth by using a fluorometer (Model 10-AU;

Turner Designs, Sunnyvale, CA, United States). Cell densities were calculated using a standard curve for each strain, although only cell densities at the surface and bottom were counted under a light microscope (Eclipse TS-100; Nikon Co., Tokyo, Japan). For sample collection during the dark period, we used a red LED flashlight (peak wavelength, 630 nm) for illumination, because red light has little effect on the DVM pattern of *Chattonella* (Shikata et al., 2013).

2.3 Monitoring DVM with a digital camera system

The system described by Shikata et al. (2016) was also used for monitoring DVM. A rectangular acrylic chamber (base: 1 cm wide × 5 cm long) containing 25 mL of cell suspension (depth, 5 cm) was held by a clamp. Each sample was illuminated by a white LED from above; the photon flux density at the water surface was adjusted to 150 µmol photons m^{-2} s^{-1}.

A monochromatic, digital, charge-coupled device camera (Pixelfly, PCO AG, Kelheim, Germany) was used to photograph the sample from the side. A long pass filter (cut off wavelength of <800 nm; LX-903, Mitsubishi Layon Co. Ltd., Tokyo, Japan) was mounted in front of the camera lens. The samples were illuminated by an infrared LED (peak wavelength, 850 nm; Pi Photonics Inc., Shizuoka, Japan) from behind, and the camera captured the light scattered by the cells. Each sample was time-lapse photographed every 15 min for 66 h (from day 0 at 18:00 to day 2 at 12:00 LT) to obtain raw data for determining the DVM. The devices that composed the system were operated in a temperature-controlled (25°C) dark room.

In the digital images, the cell density in each area is roughly reflected by its brightness. Since the brightness of a pixel in the 8-bit image is represented by 256 (2^8) steps of gray values, we first read the gray values of pixels at respective areas of cell suspension using ImageJ software (http://rsbweb.nih.gov/ij/) to evaluate vertical profiles of the cells. The surface accumulation ratios were then calculated as the common logarithm of the ratio of the average of gray values in the surface layer (0–0.75 cm) and the bottom layer (2.50–3.00 cm). Because *Chattonella* generally migrated between the surface and bottom under most experimental light conditions, the time series of surface accumulation ratios was used to represent the DVM pattern and cell accumulation. High and low ratios were recorded
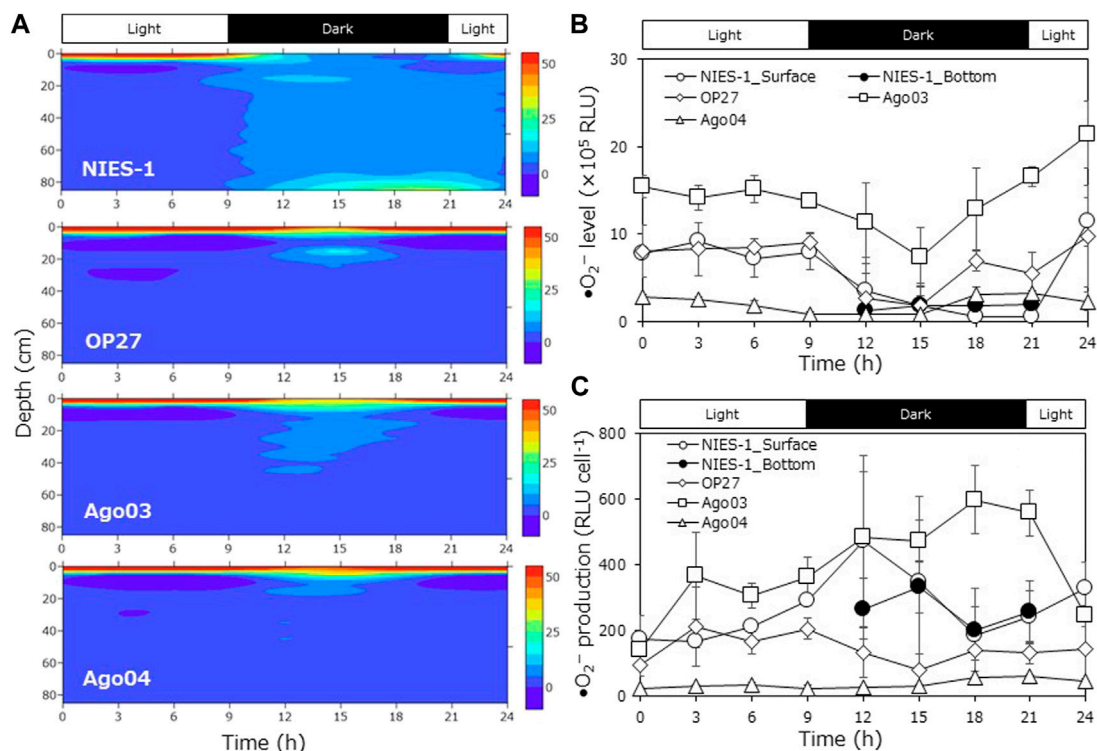
FIGURE 1
Diurnal vertical migration of different *Chattonella* strains in the cylindrical aquarium. **(A)** Time-course variations in the cell accumulation percentage at each depth layer (average of triplicate measurements), **(B)** time-course variations in superoxide ($\bullet O_2^-$) level (relative luminescence units: RLU), and **(C)** $\bullet O_2^-$ production ($\bullet O_2^-$ level per cell) of *Chattonella* strains at the surface or bottom layer (only dark periods of NIES-1) in the cylindrical aquarium. $\bullet O_2^-$ level was measured by a chemiluminescence method. Each bar represents the mean $\pm$ SD of three biological replicates.

when most cells were swimming upward and downward, respectively.

2.4 $\bullet O_2^-$ detection

$\bullet O_2^-$ was detected using the chemiluminescence reagent L-012 (FUJIFILM Wako Pure Chemical Corp., Osaka, Japan) (Nishinaka et al., 1993). The resultant chemiluminescence was monitored for 30 s using a luminometer (AB-2270 Luminescencer Octa, ATTO Corp., Tokyo, Japan). The $\bullet O_2^-$ levels in cultures were calculated by subtracting the chemiluminescence measured in the presence of 200 U of bovine superoxide dismutase (SOD; FUJIFILM Wako Pure Chemical Corp.) from the measured chemiluminescence.

2.5 Statistical analyses

The data were tested for homogeneity of variances using Levene's test. When variances were homogeneous, we used one-way analysis of variance and multiple comparisons with Tukey's honestly significant difference (HSD) test to assess the differences in *Chattonella* biological parameters among treatments. Data not showing homogeneous variances were log-transformed, and a Levene's test was performed once again. When the variances were not homogeneous even after log-transformation, we used

the Dunnet T3 test. All analyses were performed with IBM SPSS Statistics Desktop Version 19.0 for Windows (IBM Japan, Tokyo, Japan), with $p < 0.05$ indicating a significant difference.

3 Results

3.1 Patterns of DVM and superoxide production in different *Chattonella* strains

We observed DVM in four strains of *Chattonella* (NIES-1, OP27, Ago03, and Ago04) using the cylindrical aquarium. Approximately equal amounts of cells ($\sim 3.0 \times 10^5$ cells) at the late logarithmic growth phase (late log phase; 1.5–3.0×10^4 cells mL^{-1}) were injected into the aquarium. The vertical cell distribution at each time was represented by the cell accumulation ratio (%), calculated as the cell abundance at a sampling depth layer divided by the sum of cell abundances at all sampling depth layers. Average cell densities in the water column over the observation periods ranged from 2.5×10^2 to 6.1×10^2 cells mL^{-1} in the four strains (Supplementary Figure S1). It was a common trend among strains that average cell abundance in the water column gradually decreased until the middle of the dark period and then recovered. A decline in the average cell abundance might have been caused by the aggregation of cells among sampling ports, whereas an increase might have been caused by sampling and

cell division, because most *Chattonella* cells divide during the latter half of the dark period (Nemoto and Furuya, 1985).

The strain NIES-1 displayed clear DVM (Figure 1A). Most cells started downward migration at the transitional period from light to dark (at 9 h from the start time), and a portion of the cells reached the bottom during the dark period. Maximum cell accumulation ratios at the bottom were 34.6% ± 11.7% (average ±SD). Thereafter, cells rapidly migrated to the surface at the transitional period from dark to light (at 21–24 h). The cell accumulation ratio at the surface varied from 4.7% ± 1.6% to 82.0% ± 2.0% through the experimental period.

In the other strains, most cells also accumulated at the surface during the light period (Figure 1A). However, most cells continued to aggregate at the surface and scarcely reached the bottom during the dark period. Maximum cell accumulation ratios at the bottom were 2.8% ± 2.3% in OP27, 3.2% ± 1.9% in Ago03, and 0.7% ± 0.2% in Ago04; these values were significantly lower than that of NIES-1 (Turkey test; $p < 0.05$). The cell accumulation ratio at the surface ranged from 36.3% ± 1.5% to 98.6% ± 0.38% in OP27, from 36.0% ± 15.5% to 96.8% ± 0.6% in Ago03, and from 51.3% ± 6.3% to 98.2% ± 0.8% in Ago04 during the experimental period.

Levels of $\bullet O_2^-$ (relative luminescence units: RLU) and $\bullet O_2^-$ production (RLU cell^{-1}) both differed among strains (Figures 1B,C). Although levels of $\bullet O_2^-$ at the surface decreased during the dark period and then increased during the light period in all strains, the maximum $\bullet O_2^-$ production in Ago04 was significantly lower than rates in other strains (Turkey test after log-transformation; $p < 0.05$). In NIES-1 and OP27, $\bullet O_2^-$ production increased during the light period, peaked around the beginning of the dark period (9–12 h), and then decreased at the start of the light period (21 h). In Ago03 and Ago04, however, $\bullet O_2^-$ production increased during the dark period and peaked around the beginning of the light period (18–21 h). We also measured the $\bullet O_2^-$ production level at the bottom for only NIES-1 during a part of the dark period, but the value was similar to that at the surface.

3.2 Patterns of DVM and superoxide production in different growth phases and cell densities

We investigated the effects of culture growth phase and cell density on the DVM pattern within the cylindrical aquarium. The strain 4KGY was used in this experiment. Cultures at the early log phase (4.6×10^3 cells mL^{-1}) and late log phase (2.6×10^4 cells mL^{-1}) were prepared. The culture at the early log phase was injected into the aquarium. Average cell density in the water column over the observation period was 6.3×10^2 cells mL^{-1}. Next, cultures in the late log phase were inoculated into separate aquaria at three different doses (low cell density, LD; medium cell density, MD; high cell density, HD). Average cell densities in the water column in LD, MD, and HD over the observation period was 2.9×10^2 cells mL^{-1}, 1.3×10^3 cells mL^{-1}, and 2.1×10^4 cells mL^{-1}, respectively (Supplementary Figure S2). As in the interstrain comparison experiments, the average cell abundance in the water column gradually decreased until the middle of the dark period and then recovered (Supplementary Figure S2). In the HD treatment, a portion of the cells aggregated at the bottom just after cell inoculation, and

we could not sample the aggregate due to its stickiness. The average cell density in the water column did not decrease during the experimental period, meaning the aggregate scarcely increased (Supplementary Figure S2).

Cells in the early log phase displayed clear DVM (Figure 2A). Most cells started downward migration at the transitional period from light to dark (at 9 h), and a portion of the cells reached the bottom during the dark period. The maximum cell accumulation ratio at the bottom during the dark periods was 24.3% ± 12.0%. The surface cell accumulation ratio ranged from 7.7% ± 1.5% to 91.0% ± 1.9% throughout the experimental period. As with early log phase culture, cells at the late log phase at the low or medium cell density also migrated downward during the dark period. However, the maximum cell accumulation ratio at the bottom during the dark period was lower than that of the early log phase culture: 12.1% ± 3.5% at LD and 7.3% ± 1.9% at MD, although no statistically significant differences were detected (Turkey test; $p = 0.304$ for LD, $p = 0.110$ for MD). The cells did not display clear DVM at HD; cells accumulated within the upper half of the aquarium or near the bottom all day. At HD, the maximum cell accumulation ratio at the surface over the experimental period was significantly lower than in the early growth phase culture and at the other cell densities (Turkey test; $p < 0.05$).

We measured the $\bullet O_2^-$ level at the depths where cells accumulated most (surface or bottom). At LD and MD, levels of $\bullet O_2^-$ decreased during the dark period and then increased during the light period (Figure 2B). $\bullet O_2^-$ production increased during the light period and peaked during the light period (6–9 h; Figure 2C). At HD, clear rhythms of $\bullet O_2^-$ level and $\bullet O_2^-$ production were not observed. The $\bullet O_2^-$ production was very low all day, and the maximum value was significantly lower than those in other conditions (Dunnet T3 after log-transformation; $p < 0.05$).

3.3 DVM patterns and superoxide production under different nutrient conditions

We investigated the effects of nutrient deficiency on the DVM pattern using the digital camera system. Although it is difficult to completely remove nutrients from the medium based on natural seawater, the growth of *Chattonella* strains in artificial medium is not good. Therefore, we adopted the digital camera system, which requires no exchange of medium, in this experiment. Axenic strain 4KGY was incubated in medium lacking NaNO$_3$ (N-depleted medium), lacking NaH$_2$PO$_4$·2H$_2$O (P-depleted medium), or containing all components (complete medium) for 5 days before the observation of DVM. The cell densities were ~2.0×10^4 cells mL^{-1} at the start of the experiment.

Cells displayed DVM under all nutrient conditions, but surface accumulation ratios under nutrient-depleted conditions were lower than in the complete medium treatment during the light period (Figure 3). There were significant differences in the maximum moving averages of the surface accumulation ratio measured at 3-h intervals between the nutrient-depleted media and the complete medium on both days (Dunnett T3; $p < 0.05$). Moreover, to investigate the effects of nutrients on $\bullet O_2^-$ production in different *Chattonella* strains, we incubated axenic strains NIES-1
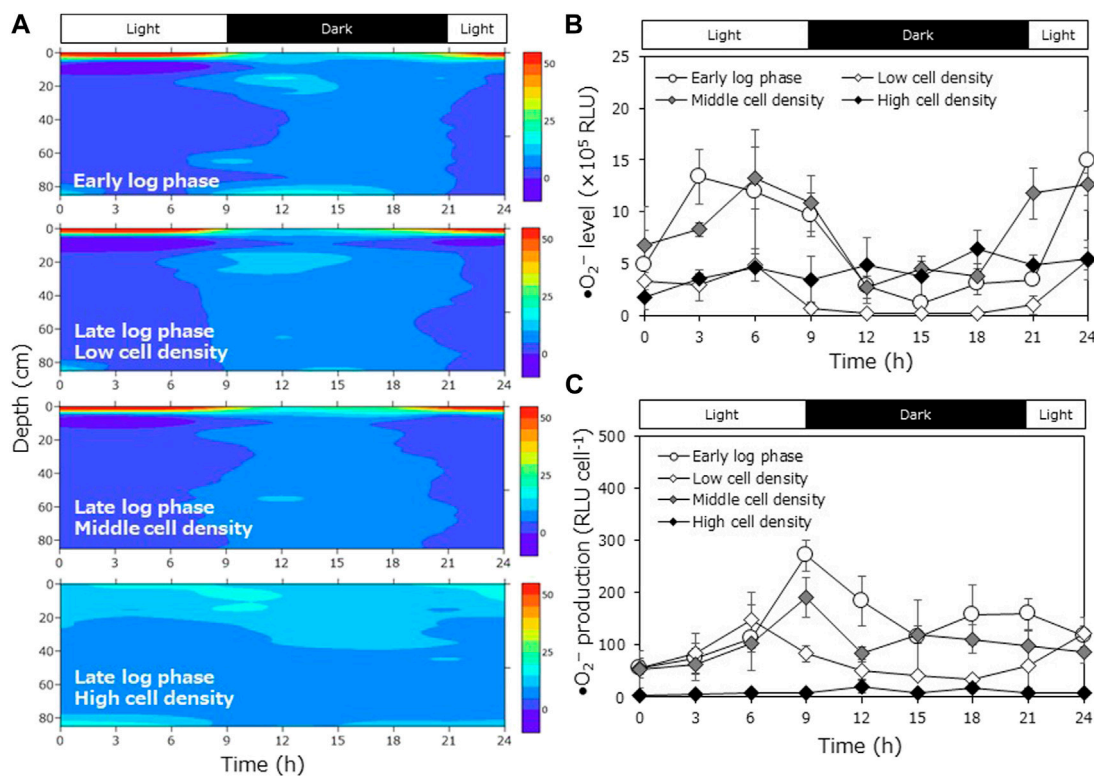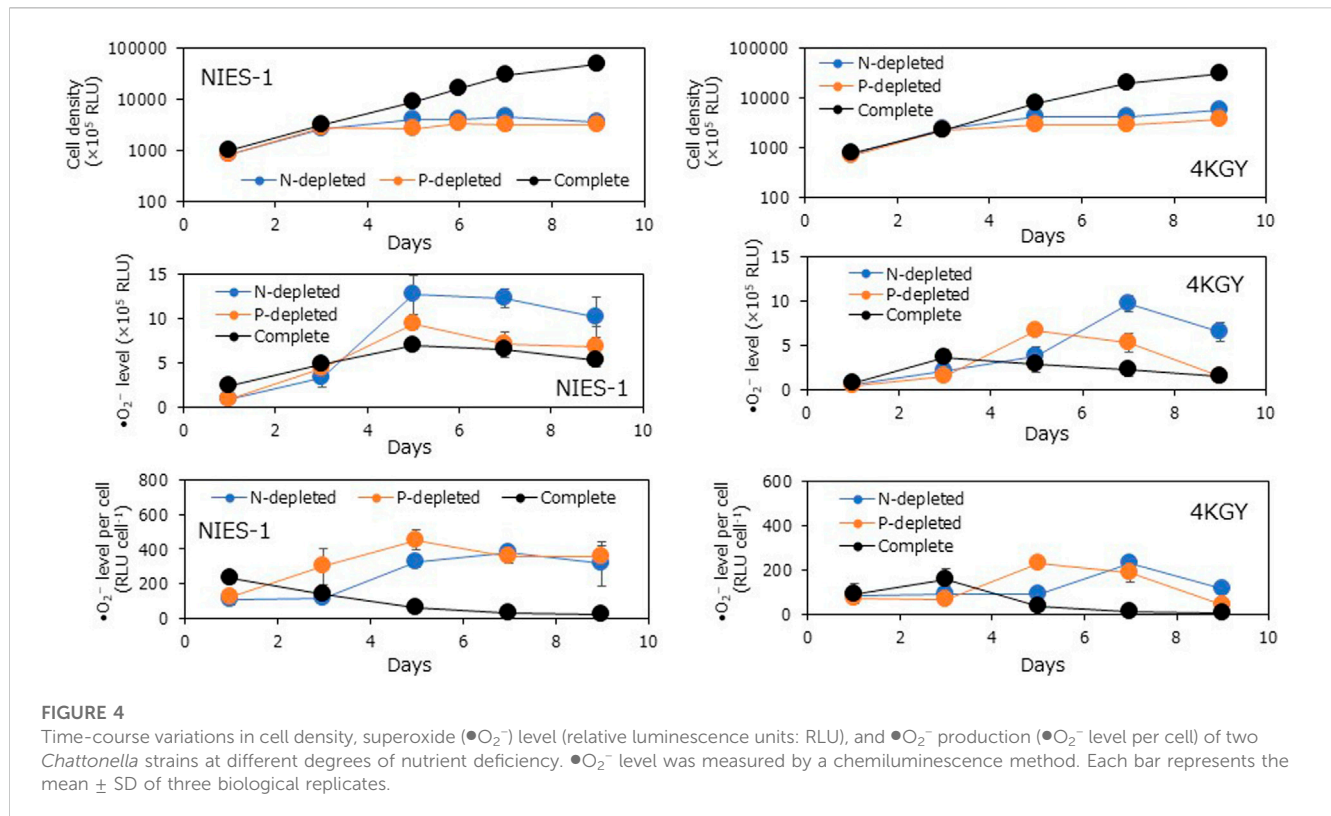
FIGURE 2
Diurnal vertical migration of *Chattonella* at different growth phases and cell densities in the cylindrical aquarium. **(A)** Time-course variations in the cell accumulation percentage at each depth (average of triplicate measurements), **(B)** time-course variations in superoxide ($\bullet O_2^-$) level (relative luminescence units: RLU), and **(C)** $\bullet O_2^-$ production ($\bullet O_2^-$ level per cell) of *Chattonella* at the surface or bottom layer in the cylinder aquarium. $\bullet O_2^-$ level was measured by a chemiluminescence method. Each bar represents the mean $\pm$ SD of three biological replicates.
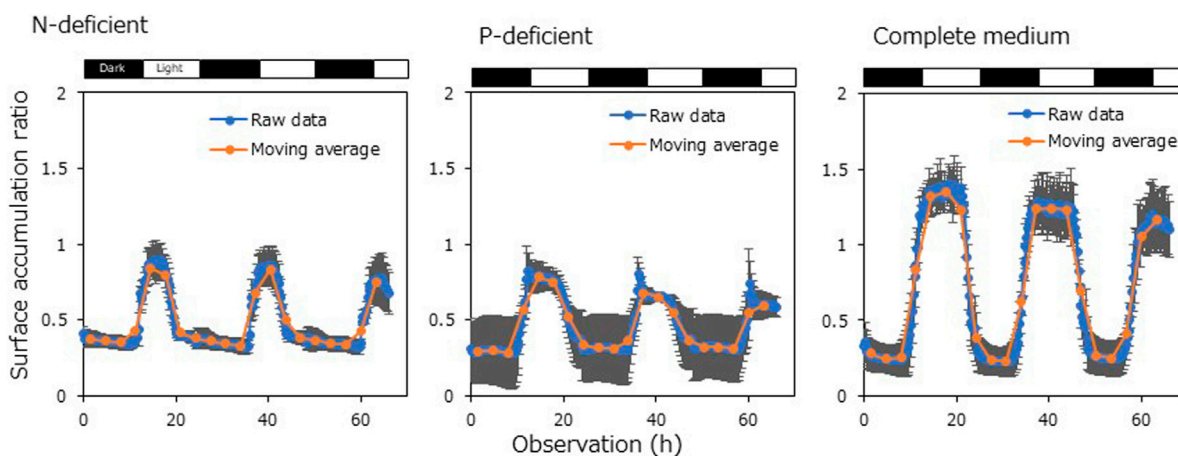
FIGURE 3
Diurnal vertical migrations of *Chattonella* at different degrees of nutrient deficiency observed by the digital camera system. Raw data and moving average at 3-h intervals are shown. Each bar represents the mean $\pm$ SD of four biological replicates.

and 4KGY in 50-mL Erlenmeyer flasks containing 25 mL of N-depleted medium, P-depleted medium, or complete medium and tracked the cell density and $\bullet O_2^-$ level for 9 days. Conditions of temperature and light were the same as in the subculture. Cells

increased throughout the experimental period in the complete medium, but increases in cell densities stopped from day 5–7 under the nutrient-depleted conditions (Figure 4). The $\bullet O_2^-$ level in NIES-1 and 4KGY cultures peaked from days 5–7 under all

FIGURE 4
Time-course variations in cell density, superoxide (●O_2^-) level (relative luminescence units: RLU), and ●O_2^- production (●O_2^- level per cell) of two *Chattonella* strains at different degrees of nutrient deficiency. ●O_2^- level was measured by a chemiluminescence method. Each bar represents the mean ± SD of three biological replicates.

conditions, but the maximum values under nutrient-depleted conditions were significantly higher than those in complete medium and that under N-depleted condition was significantly higher than that in P-depleted condition (Dunnet T3; $p < 0.05$). Production of ●O_2^- by the two strains rapidly increased on day 5 under nutrient-depleted conditions, whereas it gradually decreased from day 1 in the complete medium. The maximum ●O_2^- production by NIES-1 under nutrient-depleted conditions was significantly higher than that in complete medium (Dunnet T3; $p < 0.05$). For 4KGY, there were not statistically significant differences in the maximum ●O_2^- production among nutrient conditions, but that under nutrient-depleted conditions was significantly higher than that in complete medium on day 5 (Turkey test; $p < 0.05$) and day 7 (Dunnet T3; $p < 0.05$). The maximum ●O_2^- level and ●O_2^- production of NIES-1 were significantly higher than those of 4KGY under each condition (Dunnet T3 after log-transformation; $p < 0.05$).

4 Discussion

Among investigations conducted under quiet conditions in enclosed coastal areas or in a mesocosm, there were differences in the depth reached by a *Chattonella* red tide at night (Watanabe et al., 1995; Araki et al., 2013; Sakurada et al., 2013; Katano et al., 2014; Sakaguchi et al., 2017). In previous laboratory studies using *Chattonella* strains NIES-1 and 3KGY, most *Chattonella* cells migrated to the surface of a vessel during the light periods and to the bottom during the dark periods (Kim et al., 2005; Shikata et al., 2014). Before the present study, however, we viewed flasks

including *Chattonella* strains during the dark periods and found that some strains aggregated at the surface of the medium even during the night. The present study showed that some strains display clear downward migration during the dark periods, whereas others scarcely migrate under the same condition. Strains Ago03 and Ago04 were isolated from the same marine area during different years, and both displayed weak downward migration. Strains 4KGY used in the present study and 3KGY used in Shikata et al. (2014) were isolated from the same marine area on the same day. Compared to 4KGY (early log phase), 3KGY has higher surface accumulation ratios during the dark periods and accumulates at the bottom during the light periods in the same experimental setup, indicating that DVM in 3KGY has more entrainability. Although *Chattonella* shows variations in cell shape and toxicity among strains (Demura et al., 2009; Shikata et al., 2021), the relationship between their phenotypes (Table 1) and DVM pattern remains obscure. Our findings indicate that the strain composition of a *Chattonella* population may influence the vertical cell distribution at each time point in the field, although it is unclear what produced the interstrain differences in the DVM pattern.

Interstrain variation in the DVM pattern may contribute to species survival by decreasing the risk that all cells are exposed to a harmful environment at a certain depth. However, if only strains with a poor ability of downward migration survive, it is unclear whether the population could recover the ability. Moreover, the large diversity in DVM can inhibit densification of cells, leading to poorer competition with other microorganisms, such as antibiotic ability (Oda et al., 1992) and toxicity against other phytoplankters (Qiu et al., 2011; Fernández-Herrera et al., 2016). Therefore, the

strain composition of a *Chattonella* population may characterize the population dynamics in each marine area.

It is difficult to incubate some *Chattonella* strains at large volumes (>200 mL) in normal vessels such as an Erlenmeyer flask for days, although the reasons are unclear. Surprisingly, the present study revealed that strains OP27, Ago03, and Ago04, which can grow in large-scale incubation, displayed little downward migration. It is impossible to resuspend a cell pellet made by centrifugation of a *Chattonella* culture because the cells strongly adhere to each other at high cell density (Jenkinson et al., 2007). Although bioconvection occurs at the surface and mitigates densification during periods of upward migration, bioconvection does not occur at the bottom during periods of downward movement. Therefore, success in the large-scale incubation of *Chattonella* may be closely related to the ability of a strain to migrate downward.

Sakaguchi et al. (2017) reported that a red tide of *Chattonella* displays clear DVM when the average cell density is on the order of 10^3 cells mL^{-1} in the water column, whereas downward migration is scarcely observed when the average cell density is on the order of 10^4 cells mL^{-1} and nutrient concentrations are sufficient for *Chattonella* growth. Likewise, in the present study *Chattonella* cells scarcely displayed DVM when the average cell density in the water column (volume: 1.6 L) was more than 10^4 cells mL^{-1} (late log phase in Figure 2). Although the maximum cell density of *Chattonella* was normally on the order of 10^4 cells mL^{-1} even when the other conditions were suitable for growth, the growth phase at the time of the inoculation scarcely affected DVM patterns. Therefore, densification may hamper various physiological activities related to downward migration and growth, although the mechanism remains to be clarified. When the sample volume was small (25 mL), however, clear DVM was observed even on the order of 10^4 cells mL^{-1} (complete medium in Figure 3). In *Chattonella*, at greater incubation volume, the growth rate and maximum cell yield were lower. Thus, the effects of densification on physiological states may depend on the incubation volume in laboratory studies.

In various flagellate species, the depletion of nitrogen or phosphorus activates or inhibits DVM (Heaney and Eppley, 1980; Yuasa et al., 2018). We observed that the deficiency of nitrogen or phosphorus inhibited DVM in *Chattonella* with two axenic strains. Although the red-tide dinoflagellate *Karenia mikimotoi* aggregates at the surface all day under nitrogen-depleted conditions (Yuasa et al., 2018), we found that *Chattonella* sank more easily in nitrogen- or phosphorus-depleted conditions. In a Swedish fjord, the amount of *Chattonella* cells peaked in sediment traps deployed in deep layers (15 and 30 m depths) when a red tide of *Chattonella* was declining and nitrate concentrations in the surface layer (0–10 m depth) were low (Waite and Lindahl, 2006). In addition, DVM ceases under continuous darkness, whereas it persists under continuous red light, which acts on photosynthesis but scarcely shifts the phase of the DVM pattern (Shikata et al., 2015). Therefore, swimming would require energy from photosynthesis, which in turn requires light and nutrients, in *Chattonella*.

Kim et al. (2005) examined the relationship between the production of reactive oxygen species and DVM using the *Chattonella* strain NIES-1. They observed DVM similar to that

recorded in the present study and found that $\bullet O_2^{-}$ production was high during the light period and that it decreased during the dark period in cell-aggregated layers (surface or bottom). Yuasa et al. (2020a) observed a similar diurnal pattern in $\bullet O_2^{-}$ production in the strain 4KGY. The present study also revealed a similar pattern of $\bullet O_2^{-}$ production in the strain OP27, but the DVM pattern of strains Ago03 and Ago04 was different from that of the other strains, with $\bullet O_2^{-}$ production increasing during the dark period. Interestingly, we noticed that characteristics of the cellular $\bullet O_2^{-}$ production pattern may be categorized by cell shape in *Chattonella* strains, as noted in strains with a *Chattonella antiqua*–like shape (NIES-1, 4KGY, OP27) and strains with a *C. marina*–like shape (Ago03, Ago04); the amount of $\bullet O_2^{-}$ production, however, is not categorized by cell shape among strains (Shikata et al., 2021). These findings imply that the DVM pattern may be independent of the $\bullet O_2^{-}$ production pattern because only the latter was categorized by cell shape.

Based on experiments using the strain NIES-1, Kim et al. (2004) suggested that the growth phase (or cell density) can affect the amount of $\bullet O_2^{-}$ production but has little effect on the diurnal pattern of $\bullet O_2^{-}$ production. The $\bullet O_2^{-}$ production rate had a maximum value during the exponential growth phase (low cell density) and subsequently decreased in the stationary phase (high cell density), but $\bullet O_2^{-}$ production increased during the light period and decreased during the dark period regardless of growth phases. However, the present study using strain 4KGY showed that the diurnal pattern of $\bullet O_2^{-}$ production was less clear at higher cell density (stationary phase).

Kim et al. (2004) reported that $\bullet O_2^{-}$ production was lower when nitrogen and phosphorus concentrations were low than when these nutrients were fully supplied in strain NIES-1. On the other hand, Yuasa et al. (2020a) reported that $\bullet O_2^{-}$ production is stimulated under nitrogen- or phosphorus-deficient conditions in the 4KGY strain. Therefore, the response of $\bullet O_2^{-}$ production to nutrient deficiency appears to depend on the strain. According to the reverification result in the present study, however, $\bullet O_2^{-}$ production was stimulated under nitrogen- or phosphorus-deficient conditions in both NIES-1 and 4KGY. Previous studies have suggested that the reducing power required for $\bullet O_2^{-}$ production in the cell membrane may originate from photosynthesis, based on inhibition of $\bullet O_2^{-}$ production by the administration of a photosynthetic inhibitor during the light period as well as the increase in $\bullet O_2^{-}$ production during the light period (Marshall et al., 2002; Yuasa et al., 2020b). Yuasa et al. (2020a) have reported that $\bullet O_2^{-}$ production under nitrogen- or phosphorus-deficient conditions increase during the dark period and the extracellular levels of $\bullet O_2^{-}$ under nutrient-deficient conditions are unaffected by the presence of an inhibitor of photosynthetic electron transport—indicating that pathways of $\bullet O_2^{-}$ production other than photosynthesis exist. However, the present study revealed that diurnal patterns of $\bullet O_2^{-}$ production differ among strains. Thus, there may be differences among strains with regard to the degree of dependence on each production pathway and sensitivity to environmental conditions such as cell density and nutrient availability.

In conclusion, our findings indicate that strain, cell density, and nutrient deficiency are factors that affect the DVM pattern and $\bullet O_2^{-}$ production in *Chattonella*. Moreover, our results suggest that the diurnal patterns of vertical migration and $\bullet O_2^{-}$ production may be

independently regulated, indicating that a *Chattonella* population can have cells with numerous combinations of DVM and $\bullet O_2^-$ production patterns. A great diversity of DVM and $\bullet O_2^-$ production in a population should increase the chances of acquiring nutrients and light and successfully competing against other microorganisms in the water column. Quantitative analyses using numerical models based on the information obtained in the present study are important future tasks.

Data availability statement

The original contributions presented in the study are included in the article/Supplementary Material, further inquiries can be directed to the corresponding author.

Author contributions

TS designed this study and data analyses; TS, SK, and KY conducted experiments. All authors have read and agreed to the published version of the manuscript.

Funding

Conflict of interest

The authors declare that the research was conducted in the absence of any commercial or financial relationships that could be construed as a potential conflict of interest.

Publisher's note

All claims expressed in this article are solely those of the authors and do not necessarily represent those of their affiliated organizations, or those of the publisher, the editors and the reviewers. Any product that may be evaluated in this article, or claim that may be made by its manufacturer, is not guaranteed or endorsed by the publisher.

Supplementary material

The Supplementary Material for this article can be found online at: https://www.frontiersin.org/articles/10.3389/fcell.2023.1134227/full#supplementary-material

References

Akita, K., Yoshida, K., Noda, T., Chujo, T., Hotta, T., Shinoda, R., et al. (2022). Genetic parameter estimation for resistance to red tide raphidophyte *Chattonella antiqua* in Japanese yellowtail *Seriola quinqueradiata*. *Aquacul. Res.* 53, 4449–4459. doi:10.1111/are.15942

Araki, K., Matuoka, T., Morishita, T., and Kawasaki, S. (2013). Impacts of diel vertical migration of *Chattonella antique* (Raphidophyceae) on the benthic crustacean (*Penaeus japonicus*) in Ariake Bay. *Rep. Kumamoto Pref. Fish. Res. Cent.* 9, 13–18.

Ault, T. R. (2000). Vertical migration by the marine dinoflagellate *Prorocentrum triestinum* maximises photosynthetic yield. *Oecologia* 125, 466–475. doi:10.1007/s004420000472

Balaji-Prasath, B., Wang, Y., Su, Y. P., Hamilton, D. P., Lin, H., Zheng, L., et al. (2022). Methods to control harmful algal blooms: A review. *Environ. Chem. Lett.* 20, 3133–3152. doi:10.1007/s10311-022-01457-2

Bearon, R. N., Grünbaum, D., and Cattolico, R. A. (2004). Relating cell-level swimming behaviors to vertical population distributions in *Heterosigma akashiwo* (Raphidophyceae), a harmful alga. *Limnol. Oceanogr.* 49, 607–613. doi:10.4319/lo.2004.49.2.0607

Berdalet, E., McManus, M. A., Ross, O. N., Burchard, H., Chavez, F. P., Jaffe, J. S., et al. (2014). Understanding harmful algae in stratified systems: Review of progress and future directions. *Rev.Prog. Fut. Direct. Deep-Sea Res. II* 101, 4–20. doi:10.1016/j.dsr2.2013.09.042

Bollens, S. M., Quenette, J. A., and Rollwagen-Bollens, G. (2012). Predator-enhanced diel vertical migration in a planktonic dinoflagellate. *Mar. Ecol. Prog. Ser.* 447, 49–54. doi:10.3354/meps09467

Brand, L. E., Guillard, R. R. L., and Murphy, L. F. (1981). A method for the rapid and precise determination of acclimated phytoplankton reproduction rates. *J. Plankton Res.* 3, 193–201. doi:10.1093/plankt/3.2.193

Davidson, K., Anderson, D. M., Mateus, M., Reguera, B., Silke, J., Sourisseau, M., et al. (2016). Forecasting the risk of harmful algal blooms. *Harmful Algae* 53, 1–7. doi:10.1016/j.hal.2015.11.005

Demura, M., Noël, M. H., Kasai, F., Watanabe, M. M., and Kawachi, M. (2009). Taxonomic revision of *Chattonella antiqua, C. marina* and *C. ovata* (Raphidophyceae) based on their morphological characteristics and genetic diversity. *Phycologia* 48, 518–535. doi:10.2216/08-98.1

Fernández-Herrera, L. J., Band-Schmidt, C. J., López-Cortés, D. J., Hernández-Guerrero, C. J., Bustillos-Guzmán, J. J., and Núñez-Vázquez, E. (2016). Allelopathic effect of *Chattonella marina* var. *marina* (Raphidophyceae) on *Gymnodinium catenatum* (Dinophycea). *Harmful Algae* 51, 1–9. doi:10.1016/j.hal.2015.10.009

Gobler, C. J. (2020). Climate change and harmful algal blooms: Insights and perspective. *Harmful Algae* 91, 101731. doi:10.1016/j.hal.2019.101731

E. Granéli and J. T. Turner (Editors) (2006). *Ecology of harmful algae* (Berlin: Springer).

Harvey, E. L., and Menden-Deuer, S. (2011). Avoidance, movement, and mortality: The interactions between a protistan grazer and *Heterosigma akashiwo*, a harmful algal bloom species. *Limnol. Oceanogr.* 56, 371–378. doi:10.4319/lo.2011.56.1.0371

Heaney, S. I., and Eppley, R. W. (1980). Light, temperature and nitrogen as interacting factors affecting diel vertical migrations of dinoflagellates in culture. *J. Plankton Res.* 3, 331–344. doi:10.1093/plankt/3.2.331

Ikegami, S., Imai, I., Kato, J., and Ohtake, H. (1995). Chemotaxis towards inorganic phosphate in the red tide alga *Chattonella antiqua*. *J. Plankton Res.* 17, 1587–1591. doi:10.1093/plankt/17.7.1587

Imai, I., and Yamaguchi, M. (2012). Life cycle, physiology, ecology and red tide occurrences of the fish-killing raphidophyte *Chattonella*. *Harmful Algae* 14, 46–70. doi:10.1016/j.hal.2011.10.014

Ishimatsu, A., Sameshima, M., Tamura, A., and Oda, T. (1996). Histological analysis of the mechanisms of *Chattonella*-induced hypoxemia in yellowtail. *Fish. Sci.* 62, 50–58. doi:10.2331/fishsci.62.50

Jenkinson, I. R., Shikata, T., and Honjo, T. (2007). Modified ichthyoviscometer shows high viscosity in *Chattonella* culture. *Harmful Algae News* 35, 1–5.

Jephson, T., Fagerberg, T., and Carlsson, P. (2011). Dependency of dinoflagellate vertical migration on salinity stratification. *Aquat. Microb. Ecol.* 63, 255–264. doi:10.3354/ame01498

Kamykowski, D. (1995). Trajectories of autotrophic marine dinoflagellates. *J. Phycol.* 31, 200–208. doi:10.1111/j.0022-3646.1995.00200.x

Katano, T., Yoshida, M., Yamaguchi, S., Yoshino, K., Hamada, T., Koriyama, M., et al. (2014). Effect of nutrient concentration and salinity on diel vertical migration of

Chattonella marina (Raphidophyceae). *Mar. Biol. Res.* 10, 1007–1018. doi:10.1080/17451000.2013.879987

Kim, D., Watanabe, M., Nakayasu, Y., and Kohata, K. (2005). Changes in O_2^- and H_2O_2 production by *Chattonella antiqua* during diel vertical migration under nutrient stratification. *Aquat. Microb. Ecol.* 39, 183–191. doi:10.3354/ame039183

Kim, D., Watanabe, M., Nakayasu, Y., and Kohata, K. (2004). Production of superoxide anion and hydrogen peroxide associated with cell growth of *Chattonella antiqua*. *Aquat. Microb. Ecol.* 35, 57–64. doi:10.3354/ame035057

Kim, H. G. (2006). "Mitigation and controls of HABs," in *Ecology of harmful algae, ecological studies*. Editors E. Granéli and J. T. Turner (New York: Springer), 327–338.

Lai, Z., and Yin, K. (2014). Physical–biological coupling induced aggregation mechanism for the formation of high biomass red tides in low nutrient waters. *Harmful Algae* 31, 66–75. doi:10.1016/j.hal.2013.09.011

Marshall, J. A., Hovenden, M., Oda, T., and Hallegraeff, G. M. (2002). Photosynthesis does influence superoxide production in the ichthyotoxic alga *Chattonella marina* (Raphidophyceae). *J. Plankton Res.* 24, 1231–1236. doi:10.1093/plankt/24.11.1231

Matsusato, T., and Kobayashi, H. (1974). Studies on death of fish caused by red tide. *Bull. Nansei Reg. Fish. Res. Lab.* 7, 43–67.

McGillicuddy, D. J., Jr (2010). Models of harmful algal blooms: Conceptual, empirical, and numerical approaches. *J. Mar. Syst. J. Eur. Assoc. Mar. Sci. Tech.* 83, 105–107. doi:10.1016/j.jmarsys.2010.06.008

Nemoto, Y., and Furuya, M. (1985). Inductive and inhibitory effects of light on cell division in *Chattonella antiqua*. *Plant Cell Physiol.* 26, 669–674. doi:10.1093/oxfordjournals.pcp.a076956

Nishinaka, Y., Aramaki, Y., Yoshida, H., Masuya, H., Sugawara, T., and Ichimori, Y. (1993). A new sensitive chemiluminescence probe, L-012, for measuring the production of superoxide anion by cells. *Biochem. Biophys. Res. Commun.* 193, 554–559. doi:10.1006/bbrc.1993.1659

Oda, T., Ishimatsu, A., Shimada, M., Takeshita, S., and Muramatsu, T. (1992). Oxygen-radical-mediated toxic effects of the red tide flagellate *Chattonella marina* on *Vibrio alginolyticus*. *Mar. Biol.* 112, 505–509. doi:10.1007/bf00356297

Qiu, X., Yamasaki, Y., Shimasaki, Y., Gunjikake, H., Matsubara, T., Nagasoe, S., et al. (2011). Growth interactions between the raphidophyte *Chattonella antiqua* and the dinoflagellate *Akashiwo sanguinea*. *Harmful Algae* 11, 81–87. doi:10.1016/j.hal.2011.08.001

Roenneberg, T., Colfax, G. N., and Hastings, J. W. (1989). A circadian rhythm of population behavior in *Gonyaulax polyedra*. *J. Biol. Rhythm.* 4, 89–104. doi:10.1177/074873048900400208

Sakaguchi, M., Yamatogi, T., Hirae, S., Ishida, N., Hirano, K., and Aoki, K. (2017). Diurnal vertical migration of *Chattonella* spp. in mesocosm during a red tide in isahaya bay, nagasaki prefecture, Japan. *Bull. Plankton Soc. Jpn.* 64, 1–10.

Sakurada, K., Takahi, S., and Umemoto, T. (2013). Occuration and vertical migration of *Chattonella antiqua* in 2010 in yatsushiro sea. *Rep. Kumamoto Pref. Fish. Res. Cent.* 9, 85–90.

Sellner, K. G., Doucette, G. J., and Kirkpatrick, G. J. (2003). Harmful algal blooms: Causes, impacts and detection. *J. Ind. Microbiol. Biotechnol.* 30, 383–406. doi:10.1007/s10295-003-0074-9

Shen, M., Xu, J., Tsang, T. Y., and Au, D. W. (2010). Toxicity comparison between *Chattonella marina* and *Karenia brevis* using marine medaka (*Oryzias melastigma*): Evidence against the suspected ichthyotoxins of *Chattonella marina*. *Chemosphere* 80, 585–591. doi:10.1016/j.chemosphere.2010.03.051

Shikata, T., Kitatsuji, S., Abe, K., Onitsuka, G., Matsubara, T., Nakayama, N., et al. (2020). Vertical distribution of a harmful red-tide dinoflagellate, *Karenia mikimotoi*, at the decline stage of blooms. *J. Sea Res.* 165, 101960. doi:10.1016/j.seares.2020.101960

Shikata, T., Matsunaga, S., Iseki, M., Nishide, H., Higashi, S. I., Kamei, Y., et al. (2013). Blue light regulates the rhythm of diurnal vertical migration in the raphidophyte red-tide alga *Chattonella antiqua*. *J. Plankton Res.* 35, 542–552. doi:10.1093/plankt/fbt006

Shikata, T., Matsunaga, S., Kuwahara, Y., Iwahori, S., and Nishiyama, Y. (2016). Light spectrum regulates cell accumulation during daytime in the raphidophyte *Chattonella antiqua* causing noxious red tides. *J. Photochem. Photobiol. B Biol.* 160, 128–133. doi:10.1016/j.jphotobiol.2016.03.046

Shikata, T., Matsunaga, S., Nishide, H., Sakamoto, S., Onistuka, G., and Yamaguchi, M. (2015). Diurnal vertical migration rhythms and their photoresponse in four phytoflagellates causing harmful algal blooms. *Limnol. Oceanogr.* 60, 1251–1264. doi:10.1002/lno.10095

Shikata, T., Sakamoto, S., Onitsuka, G., Aoki, K., and Yamaguichi, M. (2014). Effects of salinity on diel vertical migration behavior in two red-tide algae, *Chattonella antiqua* and *Karenia mikimotoi*. *Plankton Benthos Res.* 9, 42–50. doi:10.3800/pbr.9.42

Shikata, T., Sakurada, K., Jomoto, Y., Oyama, N., Onji, M., Yoshida, M., et al. (2011). Growth dynamics of *Chattonella antiqua* in relation to nutrients in the Yatsushiro Sea. *Nippon. Suisan. Gakk* 77, 40–52. doi:10.2331/suisan.77.40

Shikata, T., Yuasa, K., Kitatsuji, S., Sakamoto, S., Akita, K., Fujinami, Y., et al. (2021). Superoxide production by the red tide-producing *Chattonella marina* complex (Raphidophyceae) correlates with toxicity to aquacultured fishes. *Antioxidants* 10, 1635. doi:10.3390/antiox10101635

Smayda, T. J. (1997). Harmful algal blooms: Their ecophysiology and general relevance to phytoplankton blooms in the sea. *Limnol. Oceanogr.* 42, 1137–1153. doi:10.4319/lo.1997.42.5_part_2.1137

Wada, M., Takano, Y., Nagae, S., Ohtake, Y., Umezawa, Y., Nakamura, S., et al. (2018). Temporal dynamics of dissolved organic carbon (DOC) produced in a microcosm with red tide forming algae *Chattonella marina* and its associated bacteria. *J. Oceanogr.* 74, 587–592. doi:10.1507/endocrj.EJ17-0426

Waite, A. M., and Lindahl, O. (2006). Bloom and decline of the toxic flagellate *Chattonella marina* in a Swedish fjord. *Mar. Ecol. Prog. Ser.* 326, 77–83. doi:10.3354/meps326077

Watanabe, M., Kohata, K., Kimura, T., Takamatsu, T., Yamaguchi, S. I., and Ioriya, T. (1995). Generation of a *Chattonella antiqua* bloom by imposing a shallow nutricline in a mesocosm. *Limnol. Oceanogr.* 40, 1447–1460. doi:10.4319/lo.1995.40.8.1447

Yamaguchi, M., Imai, I., and Honjo, T. (1991). Effects of temperature, salinity and irradiance on the growth rates of the noxious red tide flagellates *Chattonella antiqua* and *C. marina* (Raphidophyceae). *Nippon. Suisan. Gakk* 57, 1277–1284. doi:10.2331/suisan.57.1277

Yuasa, K., Shikata, T., Ichikawa, T., Tamura, Y., and Nishiyama, Y. (2020a). Nutrient deficiency stimulates the production of superoxide in the noxious red-tide-forming raphidophyte *Chattonella antiqua*. *Harmful Algae* 99, 101938. doi:10.1016/j.hal.2020.101938

Yuasa, K., Shikata, T., Kitatsuji, S., Yamasaki, Y., and Nishiyama, Y. (2020b). Extracellular secretion of superoxide is regulated by photosynthetic electron transport in the noxious red-tide-forming raphidophyte *Chattonella antiqua*. *J. Photochem. Photobiol. B Biol.* 205, 111839. doi:10.1016/j.jphotobiol.2020.111839

Yuasa, K., Shikata, T., Kuwahara, Y., and Nishiyama, Y. (2018). Adverse effects of strong light and nitrogen deficiency on cell viability, photosynthesis, and motility of the red-tide dinoflagellate *Karenia mikimotoi*. *Phycologia* 57, 525–533. doi:10.2216/17-61.1